Volume 12, Number 2 (April 2019) p. 288 – 307 • ISSN 1983-4195
http://dx.doi.org/10.1590/S1983-41952019000200005

REVISTA IBRACON DE ESTRUTURAS E MATERIAIS
IBRACON STRUCTURES AND MATERIALS JOURNAL

Experimental studies of short concrete reinforced steel fiber beams under bending

Estudo experimental de vigas curtas de concreto com fibras de aço sujeitas à flexão

H. L. HERSCOVICI [a]
helena_lh25@hotmail.com
https://orcid.org/0000-0002-0828-893X

D. ROEHL [a]
droehl@puc-rio.br
https://orcid.org/0000-0003-4644-120X

E. DE S. SÁNCHEZ FILHO [b]
emilsanchez@uol.com.br
https://orcid.org/0000-0001-6749-9967

Abstract

This paper presents the results of a test program on 24 concrete beams with a cross section of 15 x 15 cm. Those are divided into two groups of 12 beams. Group I has a steel fiber content of 40 kg/m³ while Group II uses 60 kg/m³ of steel fibers. The tests consider three sets of beam lengths: 300 mm, 500 mm and 800 mm. The beams were submitted to bending aiming at investigating shear stresses, bending, strain energy, toughness, scale effect and fracture energy. Group II showed a slightly higher resistance to rupture than Group I. However, the smaller the length, the larger the influence of the fiber content. The largest fiber content gave the concrete higher resistance when submitted to bending and shear, especially for the smaller lengths. Both strain and fracture energy, however, show considerable differences for smaller lengths, but are almost the same for the 800 mm beams. Toughness shows improvement in the longer beams and a reduction of this property in the shorter beam from Group II.

Keywords: bending, concrete, steel fibers.

Resumo

Este estudo apresenta os resultados do rompimento de dois grupos de vigas de concreto com fibras de aço. Cada grupo foi composto de 4 vigas com vão de 300 mm, 4 com vão de 500 mm e 4 com vão de 800 mm e seção de 15 cm x 15 cm. A variação dos grupos se deu pela quantidade de fibras (I com 40 kg/m³ e II com 60 kg/m³). Foram avaliados o comportamento da tensão tangencial, momento de fendilhação, energia de deformação, tenacidade, efeito escala e energia de fratura. O grupo II apresentou maior resistência máxima, sendo essa diferença pouco significativa, entretanto, quanto menor o vão maior a influência das fibras. O maior consumo de fibras conferiu à matriz maior resistência à flexão e à tensão tangencial, tendo maior influência nos vão menores. Tanto a energia de deformação quanto a energia de fratura apresentam diferenças consideráveis para os vãos menores, chegando quase a se igualar nos dois grupos para o vão de 800 mm. A tenacidade aumentou mais nas vigas de maior vão e sofreu maior redução para o menor vão do grupo II.

Palavras-chave: flexão, concreto, fibras de aço.

[a] *PUC-Rio, Civil Engineering Department, Rio de Janeiro, RJ, Brazil;*
[b] *UFF, Civil Engineering Department, Rio de Janeiro, RJ, Brazil.*

Received: 09 Mar 2017 • Accepted: 22 Fev 2018 • Available Online:

1. Introduction

Reinforced concrete is the most used material in the civil construction field currently. This fact is due to the advantages that the material offers and the improvement that has been made over the years. However, reinforced concrete also has a downside in its use and one of the disadvantages is the low ductility and therefore it causes shorter life cycle of the structures and faster collapse after the first signs of fracture or other pathologies.

The complement of fibers to concrete aims to decrease the characteristic brittleness of the conventional material providing better tensile strength and ductility, therefore, there is a reduction of fracture in the material. There are several fiber types that can be added to concrete with this purpose. Some of them are steel, polypropylene and nylon. The fiber must be chosen according to the needs of the work in demand.

Fibers are important in fracture control, because when the material cracks, fibers make it possible to pass the tension by the fractures to the concrete matrix. For the last five decades, steel fibers are the most used ones in order to improve concrete characteristics. The upsides of steel fibers are its low cost and the fact that it doesn't jeopardize significantly concrete consistency, an important factor to this material workability. Several experimental studies were made to evaluate the increase of strength and ductility due to steel fiber reinforcement to the concrete mix. Barros et al [1] claims that the main concrete property improved by steel fibers is the energy absorption capacity. According to Maidl [2] the most important improvement made by steel fibers is to avoid crack spreading and improve their distribution throughout the concrete matrix. Marangon [3] presents studies with self compacting concrete with steel fibers that shows significant improvement of concrete ductility. Lappa et al. [4] presents test results of high resistance concrete beams reinforced with steel fibers under bending for cyclic and static loading that evaluates the consumption of fibers in the peak load. Those studies show positive influence of steel fibers on strength and ductility of the material in experiments under static loadings, showing that a higher fiber volume improves strength to load capacity. Their results for cyclic loadings require a mixture with better workability to get more trustful data. Yaziki et al. [5], Karahan et al. [6], Wang et al. [7] introduce data about the effect of fiber concentration and their dimensions in the reinforced concrete matrix, indicating that a higher concentration of fibers helps lower the costs and improves tensile and flexural strength. Recently, the work of Toledo FIlho et al. [8] presents positive results increasing tensile strength in self compacting concrete blocks, showing that steel fibers helps improve the efficiency of stress transfer among the concrete mix and steel bars in addition to increasing the ductility of the element.

This paper aims to present the test results of Herscovici [9] in an experiment with 24 steel fiber reinforced concrete beams under bending, in which the beams were divided in two groups according to the fiber consumption adopted. There were beams with three different spans to evaluate scale effect and 10 specimens for each group, for concrete control purposes.

The experiment took place in the "Laboratório de Estruturas e Materiais do Departamento de Engenharia Civil" in PUC – Rio (LEMDEC).

The bending tests results are interpreted and used to evaluate the influence of fiber consumption in strain energy, toughness and fracture energy and the improvement of tensile strength of steel fiber reinforced concrete. Scale effect is also approached.

2. Experimental program

Bending tests were made to evaluate toughness in steel fiber reinforced concrete beams. Aiming to study scale effect, the beams were constructed with the same cross section (150 mm x 150 mm) and three different spans (300 mm, 500 mm and 800 mm)

Beams were divided in two groups:

- Group I: compressive strength 30 MPa and fiber consumption of F1=40 kg/m³.
- Group II: compressive strength 30 MPa and fiber consumption of F2=60 kg/m³.

Beams with same span and same fiber volume were separated by series. Table 1 indicates groups' specifications.

Each group was formed by 12 beams, four beams to each span and 10 specimens were built, in a total of 24 beams and 20 specimens. Two concrete mixes were made, one for each group, and the 10 specimens made had the purpose of concrete control, 4 of them for compression tests, three for diametrical compression tests to evaluate tensile strength and three to evaluate the modulus of elasticity for each group.

To identify the beams, the following names were employed

Beams: LX-Y-VZ, being X the span in mm, Y the fiber consumption in kg/m³, V to make reference to the beams and Z indicates the number of the beam.

For instance, L500-60-V4 corresponds to the 500 mm span, 60 kg/m³ of fiber consumption and 4 indicates the 4th beam built.

Specimens: CPK-GW, CP indicates it's a specimen, K is the number of the specimen, G indicates "group" and W the group number.

For instance, CP7-G2 corresponds to the 7th specimen of the group II.

The concrete was mixed in the same laboratory as the tests. Concrete had a pre estabilished dosage (1:1.48:1.65:0.45 – cement : sand : gravel : water/cement factor), aiming to achieve a minimum compressive strength of 30 MPa.

Table 1
Groups' specifications

	Fiber volume (kg/m³)	Number of beams	Beam's cross section (mm)	Spans (mm)	Specimens
Group I	40	12	150 x 150	4 of 300; 4 of 500; 4 of 800	10
Group II	60	12	150 x 150	4 of 300; 4 of 500; 4 of 800	10

Table 2
Beams' test schedule

Group	Series	Beam	Test date	Concreting date	Days until test
I	Series L800-40	L800-40-V1 L800-40-V2 L800-40-V3 L800-40-V4	06/10/2015	01/09/2015	35
	Series L500-40	L500-40-V1 L500-40-V2 L500-40-V3 L500-40-V4	13/10/2015	01/09/2015	42
	Series L300-40	L300-40-V1 L300-40-V2 L300-40-V3 L300-40-V4	13/10/2015	01/09/2015	42
II	Series L300-60	L300-60-V1 L300-60-V2 L300-60-V3 L300-60-V4	14/10/2015	08/09/2015	36
	Series L500-60	L500-60-V1 L500-60-V2 L500-60-V3 L500-60-V4	20/10/2015	08/09/2015	42
	Series L800-60	L800-60-V1 L800-60-V2 L800-60-V3 L800-60-V4	20/10/2015	08/09/2015	42

2.1 Materials

The cement used was the CP-II-F-32, sand's maxim characteristic dimension was Dmax ≤ 4.75 mm and fineness modulus was 2.6 mm, obtained by standardized tests. The large aggregate was the gravel type "0" with maxim characteristic dimension of 9.5 mm, obtained by tests following NBR 7217/87 [10] and NBR 9937/87 [11]. To improve concrete workability a super plasticizing additive was employed, the ADVA FLOW 20 A. The steel fibers used in the concrete mix were Dramix RL 45/30 BN fibers from Bekaert. For concrete control tests, the machine used was the universal press MTS from LEM – DEC of PUC-Rio with 500kN load capacity. Table 2 shows concreting and tests schedule.

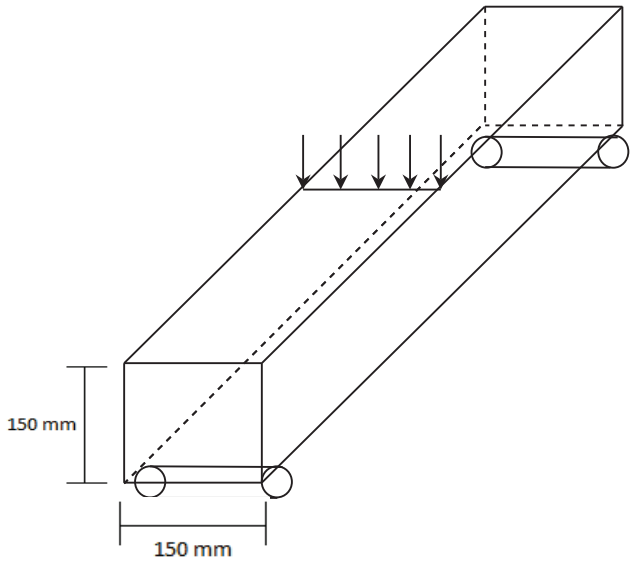

Figure 1
Bending test

2.2 Test methods

24 beams were submitted to bending tests in the scheme presented in Figure 1, following instructions of ASTM C1018/97 [12], with third loading point in the middle of the span. The supporting points were fixated 3 cm away from the far ends of the beams.
To run the bending tests, an adapted portico was connected to the MTS machine with 1000 kN capacity, as shown in Figure 2. The machine was operated so the deflection of the center point was in a constant rate of 0.1 mm/min, following the instructions in ASTM C1018/97 [12]. The bending tests allowed collecting data concerning the first crack and partial data from residual strength.

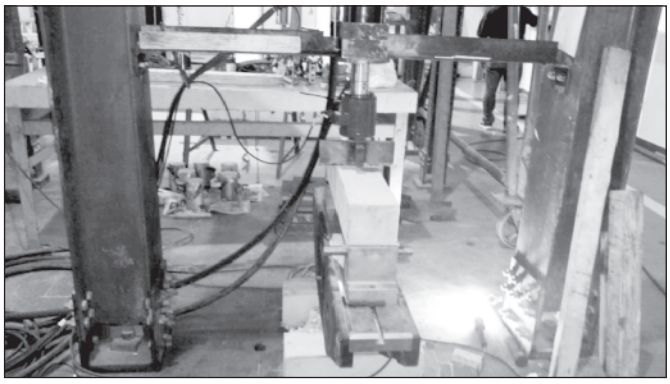

Figure 2
Adapted frame for bending tests in MTS universal machine

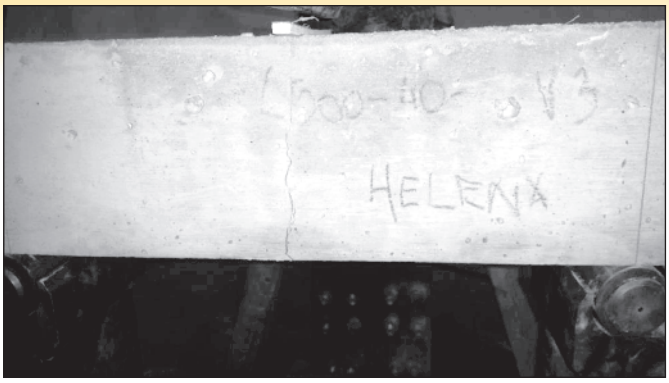

Figure 3
First cracks' behavior in tested beams

First cracks presented themselves in a similar way as shown in Figure 3. Deflection data were obtained by software directly connected to the machine used.

3. Results analysis

The concrete mix made to represent group I showed an average compressive strength of f_c = 39.25 MPa, and the one made for group II, f_c = 39.96 MPa. Tensile strength for group I was $f_{tD,m}$ = 2.56 MPa and for group II $f_{tD,m}$ = 2.73 MPa. Modulus of elasticity values were E_{ci} = 27.58 GPa concerning group I and E_{ci} = 25.60 GPa, group II. Table 3 shows individual results for each specimen to obtain average compressive strength values, Table 4 for tensile strength and Table 5 for the modulus of elasticity.

3.1 Maximum strength's percentage increase analysis

There was a percentage increase of maximum strength with fiber addition. An analysis was made of the percentage increase of the maximum resistance of group II relative to group I according to the span of the beam. The 300 mm span beams showed an increase of resistance in the range of 35% in group II comparing to group I. The ones with span of 500 mm, 30% and the ones with 800 mm, an increase of 24%. Figure 4 shows a chart representing this situation. Regarding the effectiveness of the fibers, the larger the span, less effective are the fibers in increasing strength.

3.2 Tangential stress analysis

Tangential stress is defined by:

$$\tau = \frac{P}{bh} \quad (1)$$

Table 3
Concrete compressive strength

Group	Specimen	Test	Maximum load (kN)	Days until test
I	CP7-G1	Compression	310.22	39.25
	CP8-G1		327.33	
	CP9-G1		284.06	
	CPR-G1 (10)		311.34	
II	CP7-G2	Compression	306.84	39.96
	CP8-G2		314.99	
	CP9-G2		330.91	
	CPR-G2 (10)		302.54	

Table 4
Specimens' tensile strength

Group	Specimen	Test	Maximum load (kN)	Tensile strength (MPa)
I	CP1-G1	Compression	100.04	3.18
	CP2-G1		68.91	2.19
	CP3-G1		72.25	2.30
II	CP1-G2	Compression	96.13	3.06
	CP2-G2		76.77	2.44
	CP3-G2		84.53	2.69

Table 5
Compressive strength values obtained in elasticity modulus tests

Group	Specimen	Test	Maximum load (kN)	E_{ci} (GPa)
I	CP4-G1	Elasticity modulus	300.11	27.58
	CP5-G1		307.39	
	CP6-G1		309.21	
II	CP4-G2	Elasticity modulus	221.51	25.60
	CP5-G2		318.53	
	CP6-G2		259.07	

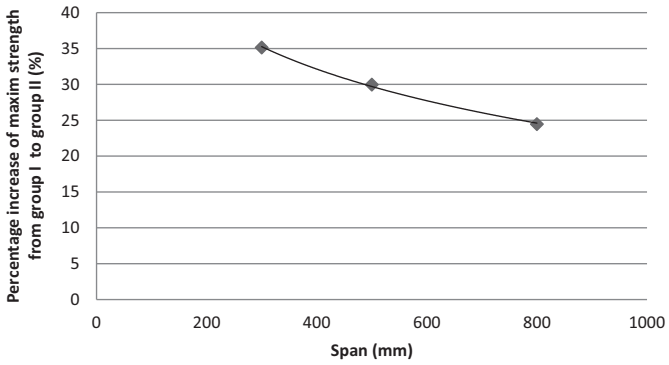

Figure 4
Percentage increase of maxim strength comparing group I to group II according to span

in which
τ – tangential stress (MPa);
P – load correspondent to first crack (kN);
b – beam width (m);
h – beam height (m).
Tangential stress analysis considers the ratio $\frac{a}{h}$, in which a stands for half of the span between supports (the whole span subtracted 3 cm from each side to provide stability to the beam) and h = 0.15 m for all spans of beams (cross section 0.15 m x 0.15 m). Figure 5 shows that as $\frac{a}{h}$ increases, tangential stress decrease. The difference between tangential stresses from group I and group II decreases as the ratio increase. Table 6 presents the results of the ratios between tangential stresses from groups I and II.

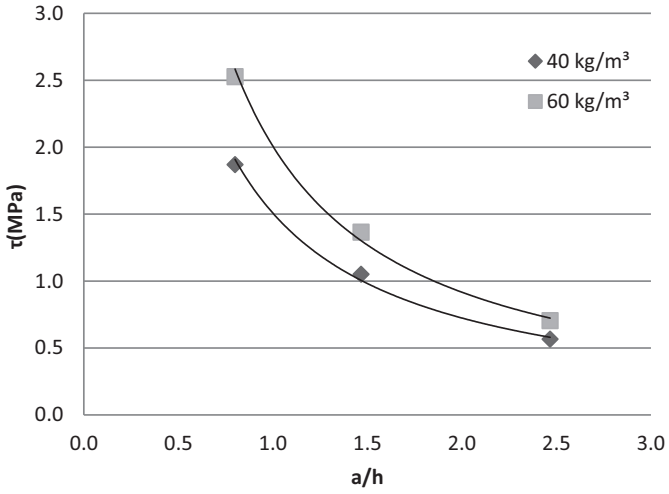

Figure 5
Tangential stress x ratio a/h for average stress values

Table 6
Ratios between tangential stresses

a/h	$\Delta = \tau_{40}/\tau_{60}$
0.80	0.74
1.47	0.77
2.47	0.80

3.3 Cracking moment analysis

Cracking moments are defined by:

$$M = \frac{Pa^2}{l} \quad (2)$$

$$\varphi = \frac{\delta}{a} \quad (3)$$

where
M – cracking moment (kN.m);
P – load correspondent to first crack (kN);
a – half of the span between supports (m);
l – beam's span (m).
ϕ – rotation correspondent to cracking moment;
δ – deflection correspondent to first crack (m).
Figure 6 presents the average values of cracking moments and respective rotation for each series. As the fiber consumption raises the cracking moment shows higher values. Rotation for groups I and II have similar values. In the series with span of 300 mm and 500 mm there is a small difference in rotation values and a significant increase of the corresponding cracking moment, while the series with 800 mm span shows more significant increase of rotation for the same moment behavior. Table 7 presents the ratio

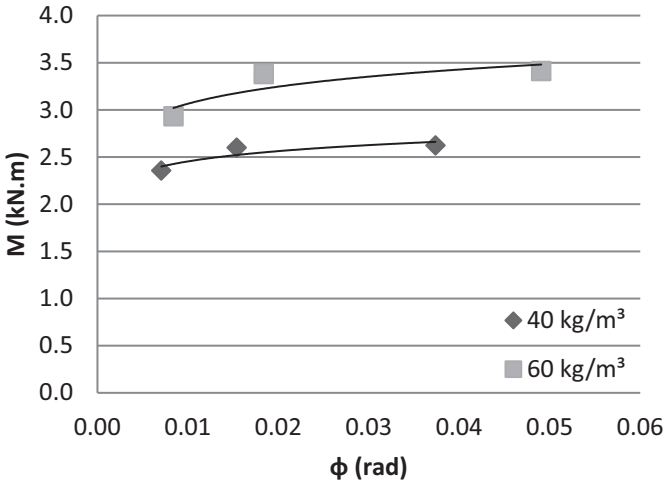

Figure 6
Cracking moment x rotation for average values in each series

Table 7
Ratio between cracking moments according to the span

Span (mm)	Δ_1
300	1.30
500	1.30
800	1.24

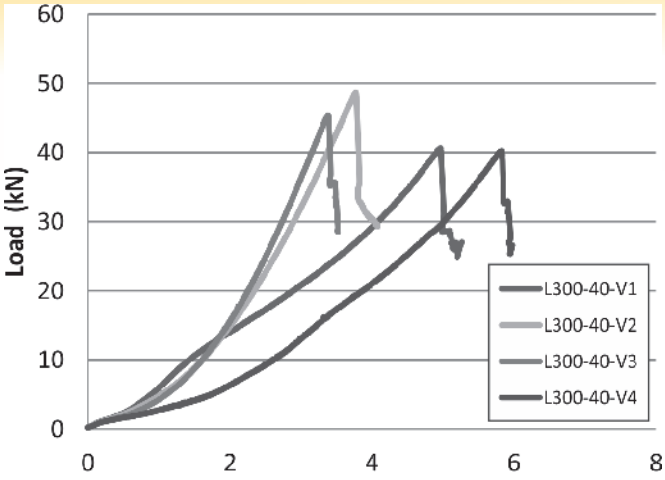

Figure 7
Graph load x deflection: 300 mm span in group I

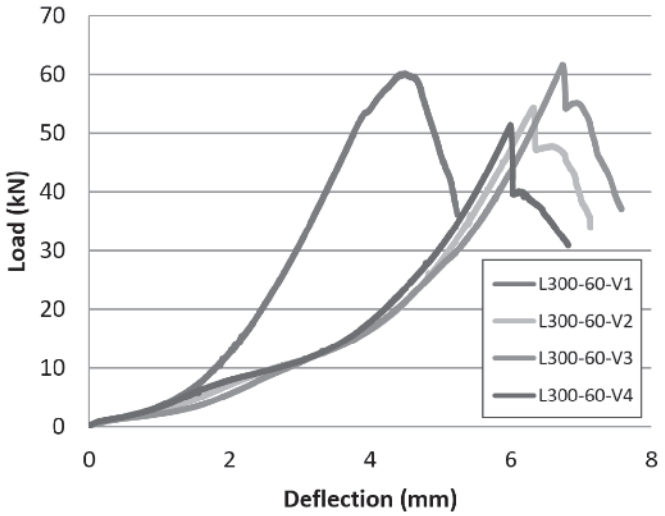

Figure 8
Graph load x deflection: 300 mm span in group II

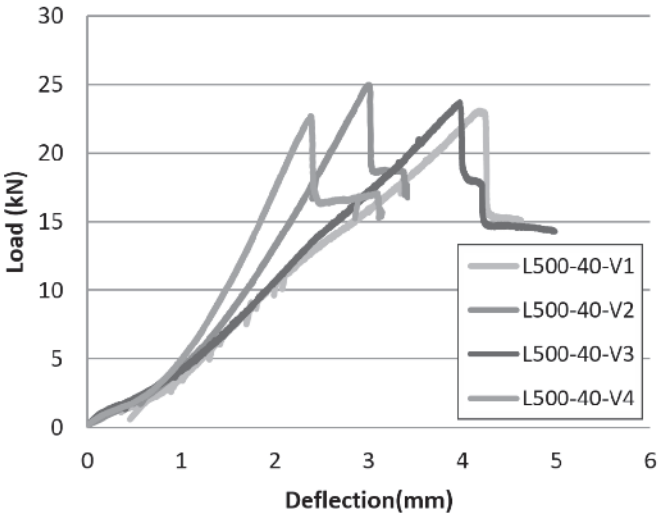

Figure 9
Graph load x deflection: 500 mm span in group I

between moments according to fiber consumption for each span, being $\Delta_1 = \frac{M_{60}}{M_{40}}$ the ratio between cracking moments from gourp I and group II. There's a reduction in the ratio between moments as the span grow. Results of this ratio correspondent to the 300 mm and 500 mm spans are very similar, however, regarding the 800 mm span, there is a more significant reduction. The greater the span, the greater the cracking moment for the corresponding loads. Fracture occurs more easily in larger spans, therefore, the ductility of the element wears off as the span increase.

3.4 Strain energy analysis

Strain energy E_{def} is defined by the area below the chart load x deflection and its unit is Joule (J).
Strain energy values were taken from the graphics using Simpson's method, analyzed point by point from the tests records. The graphs "load x deflection" for the beams with 300 mm span are represented in Figure 7 and Figure 8, beams with 500 mm span in Figure 9 and Figure 10 and the 800 mm span beams in Figure 11 and Figure 12. In this chapter there is a beams' elastic zone's work analysis. It's noticeable a marked decrease of the strain energy as the ratio $\frac{a}{h}$ grows.

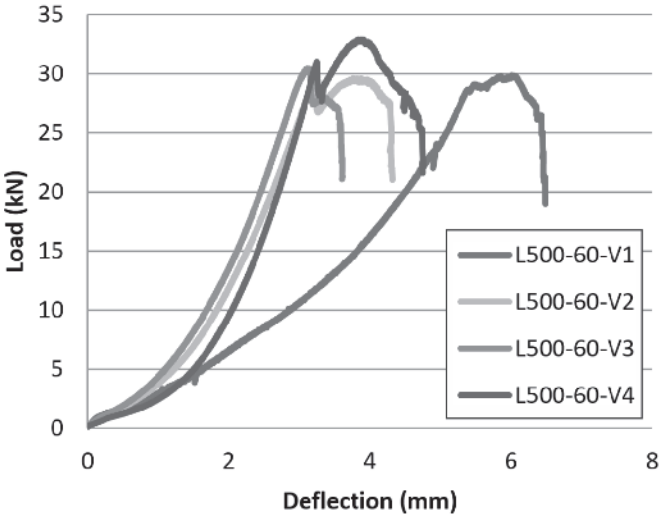

Figure 10
Graph load x deflection: 500 mm span in group II

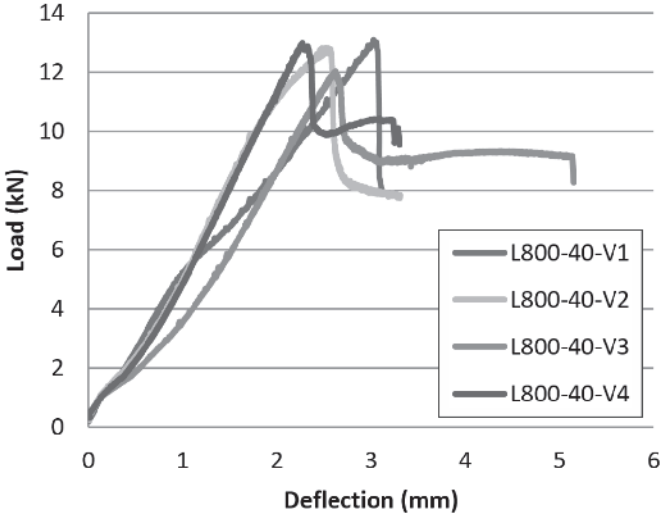

Figure 11
Graph load x deflection: 800 mm span in group I

Group II showed a more significant decrease than group I. Another relevant fact for strain energy analysis is the similarity of the curves on the larger span corresponding points ($\frac{a}{h}$ = 2.47 ratio or L = 0.8m). The chart in Figure 13 show a less effective contribution of the fibers as the span gets bigger.

3.5 Toughness analysis

The parameter used to analyze toughness is the flexural toughness factor (FT) calculated as shown in JSCE – SF4 (1984) [13] by:

$$FT = \frac{T_b}{\delta_{tb}} \times \frac{L}{bh^2} \quad (4)$$

where
FT – flexural toughness factor (MPa);
L – span (mm);
b – cross section width (m);
h – cross section height (m) ;
T_b – flexural toughness (area under the "load x deflection" curve) limited to the point corresponding to δ_{tb};
δ_{tb} – deflection corresponding to L/150 (mm).

Beams with 800 mm span of group II didn't achieve the appropriate deflection to calculate FT for this series. For toughness analysis purposes some values normally extracted from the graphs "load x deflection" were assumed based in the standard behavior of the beams. For the 800 mm span, T_b values are relative to a deflection of δ_{tb} = 4.93 considering Just the span between supports. Some approximations of missing toughness values were necessary to analyze this parameter in all spans tested. The approximations were made based on the behavior of the material and the last displacements taken by the machine during tests. Values of corresponding loads were assumed in the displacement needed to analysis. Average values of flexural toughness are presented in Figure 14.

Regarding flexural toughness an increase of energy absorption capacity is noted as the span grows. Table 8 presents the ratio $\Delta_2 = \frac{M_{60}}{M_{40}}$ for all spans.

Concerning beams with 300 mm span, the ones with fiber consumption of 60 kg/m³ show less energy absorption capacity, being around 70% of the energy absorption capacity of the ones with 40 kg/m³. Beams with 500 mm also present a decrease of energy absorption capacity in group II, but less significant, being around 90% of group I's capacity. Beams with 800 mm span

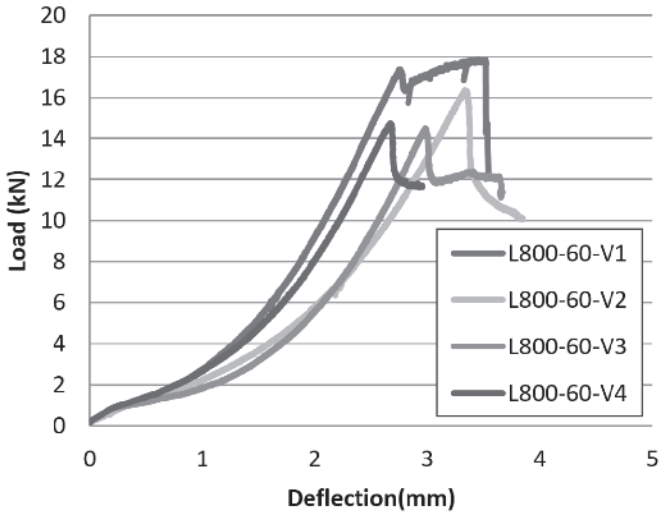

Figure 12
Graph load x deflection: 800 mm span in group II

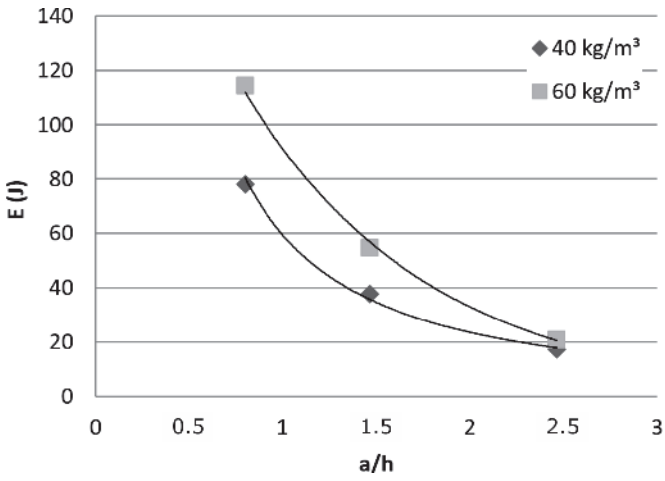

Figure 13
Strain energy x ratio a/h for average work values for each span in each group

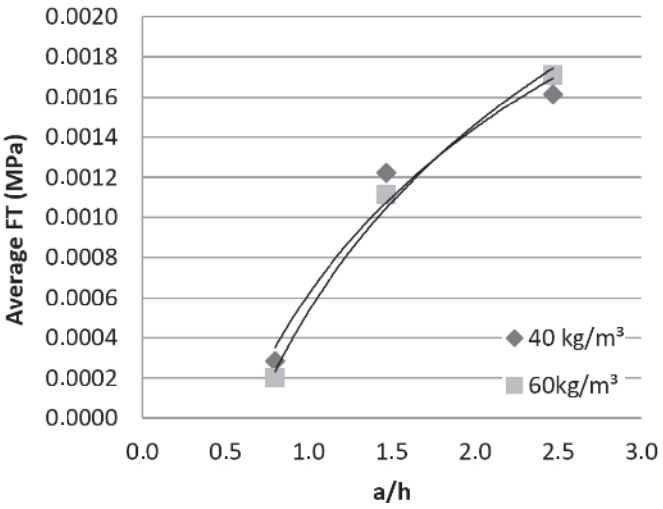

Figure 14
Average FT x ratio a/h for flexural toughness in each series

Table 8
Ratio between flexural toughness factors in group I and group II

a/h	Δ_2
0.8	0.7127
1.47	0.9099
2.47	1.0578

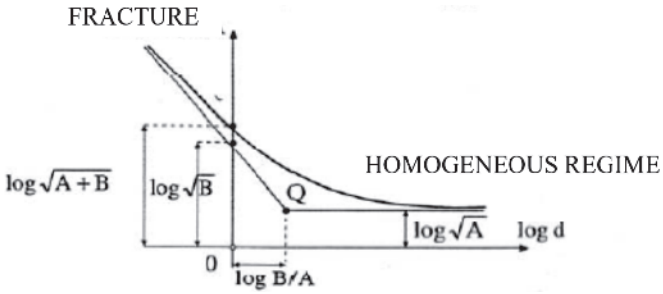

Figure 15
MSFL's diagram. CARPINTERI *et al* (1995)

present a different behavior, showing a better energy absorption capacity in Group II instead of group I, although the difference is really small, beams in group II show higher flexural toughness factor than in group I. That could implicate that, as the span grows, the fiber volume can improve the concrete mix, although due to lack of tests with larger spans it inconclusive if fibers can or cannot improve concrete toughness as the span and fiber consumption both rise.

3.6 Scale effect

By "Multifractal Scaling Law" (CARPINTERI et al., 1995) [14]:

$$\sigma_n = \sqrt{A + \frac{B}{d_c}} = f_t \sqrt{1 + \alpha_0 \frac{d_{max}}{d_c}} \quad (5)$$

where
σ_n – tensile strength;
f_t – lowest nominal tensile strength;
d_c – characteristic structure dimension;
A,B – physical constants;
d_{max} – aggregate's maxim dimension;
α_0 – empirical constant.

Figure 15 shows how MFSL works and indicates dimension range for wich scale effect is significant. As "d" grows, tensile strength tends to a constant and different from zero value. Otherwise when d tends to zero, tensile strength tends to infinity, limiting scale effect. When structure dimensions present d > B, scale effect tends to disappear. An example is the rupture as soon as fracture process begins. When d < B, scale effect is significant.

Scale effect results for both groups are presented in Figure 16 comparing to the MFSL. Tensile strength under bending is calculated by:

$$f_{ctm} = \frac{3}{2}\frac{Pl}{bh^2} \quad (6)$$

where
f_{ctm} – tensile strength under bending in one cutlass (MPa);
P – rupture load (N);
l – length (mm);
b – cross section width (mm);
h – cross section height (mm);
MFSL's was analyzed assuming α_0 = 0.3.

Comparing test results and Carpinteri's expression it can be said that scale effect presents itself in this study. Analysis show a linear decrease of tensile strength as the span grows for both groups.

3.7 Fracture energy

Critical stress factor K_{IIc} is used to measure fracture energy. It can be calculated by:

$$K_{IIc} = \sqrt{\frac{E_{ci} G_{II}}{1 - \nu^2}} \quad (7)$$

where
K_{IIc} – critical stress factor ($\frac{kN}{m^{3/2}}$);
E_{ci} – elasticity modulus (kPa);
G_{II} – fracture energy by surface unity (kN/m);
ν – Poisson's coefficient.

Poisson's coefficient couldn't be achieved by experimental data because transversal displacements weren't measured during tests. Considering that Poisson's coefficient varies between ν = 1/6 and ν = 1/5, critical stress factor was analyzed considering this variegation.

For this analysis five values between the range were picked to calculate critical stress factor. K_{IIc} values stay almost the same when Poisson's coefficient varies, presenting a less than 1% increase in the considered range. The curve for each series is shown in Figure 17.

As span grows, fiber effectiveness decrease. This fact shows that energy absorption capacity reduces, which make structures more fragile. Bigger spans raise even more the element's fragility.

4. Conclusions

Based on experimental results analysis the following conclusions were reached.

All beams show increase in maximum rupture load value in the group with higher fiber consumption. As the span gets larger, fiber influence reduces.

Resistance to rupture increase showed a non uniform behavior.

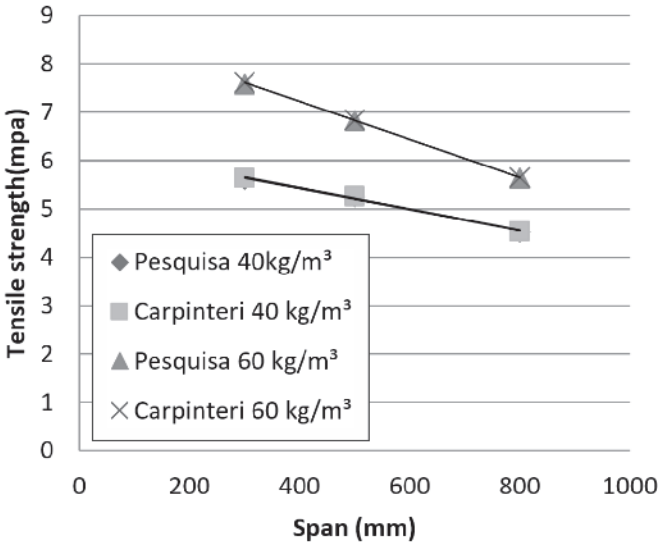

Figure 16
MFS law x research's results for 40 kg/m³ and 60 kg/m³ fiber consume

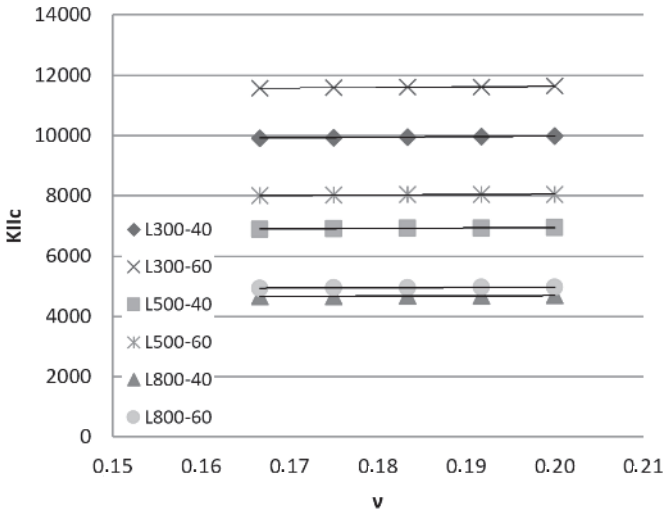

Figure 17
K_{IIc}'s variation according to Poisson's coefficient

As span grew, the resistance to rupture increased in a lower rate. Comparing group II to group I, beams with 300 mm span enhanced resistance in 35%, the ones with 500 mm in 30% and the ones with 800 mm spans were only 24% more resistant to rupture in group II, showing influence of span size in resistance increase.

As the ratio $\frac{a}{h}$ increases, tangential stress shows a decrease in both groups. When $\frac{a}{h}$ = 0.8 the ratio between both tangential stresses is $\Delta_{0.8} = \frac{\tau_{40}}{\tau_{60}} = 0.74$, when $\frac{a}{h}$ = 1.47, $\Delta_{1.47}$ = 0.77 and $\Delta_{2.47}$ = 0.8 when $\frac{a}{h}$ = 2.47. These results show that higher fiber volume is less effective in tangential stress when span rises.

Cracking moment is also affected by fiber consumption. Beams from Group II got between 24% and 30% (depending on the span) higher resistance values when submitted to bending than beams in Group I. As span rises there is a more significant drop in cracking moment values. Analyzing smaller spans, there isn't a significant difference on the ratios between the moments. This data indicates that, as the span gets smaller the ratio between moments should be constant around 1.30. The group with higher fiber consume showed results slightly bigger regarding cracking moment for the largest span, but the difference stayed around 3% to 4%, comparing to smaller spans, even though ratio between moments was a little higher than both smaller spans.

Strain energy E_{def} presents a uniform behavior analyzing the variegation of ratio $\frac{a}{h}$. Stored energy gets lower as span grows. Fibers affect strain energy in the bigger span (ratio $\frac{a}{h}$ = 2.47) very little, considering that the curves of the two groups are almost overlapping in the point corresponding to this ratio. Fibers can make the material store more energy, although, as span grows they lose their effectiveness and raising fiber consumption tends not to matter to improve this characteristic of the material.

Energy absorption capacity measured by flexural toughness factor increases when span rises in both groups. Although, toughness increase varies in a non linear curve and shows a divergent behavior comparing groups I and II. Group I presents higher flexural toughness values for 300 mm and 500 mm spans, but for 800 mm span, flexural toughness was higher in group II but the difference between flexural toughness factors in both groups was small. When it comes to toughness, results show a more relevant influence of the span instead of fiber consumption. Higher fiber volume showed smaller flexural toughness factor value in smaller length beams. BARROS (1995) [15] says that fiber complement benefits mainly energy absorption capacity, however, his studies did not predict scale effect.

Scale effect is noted in this study. The proximity of the data analysis with the ones calculated by the multifractal scale law method corroborate with this conclusion.

Regarding fracture energy, fibers have more influence in smaller spans' beams. Poisson's coefficient does not show a significant relevance in concrete when its value varies for the range used in this study.

5. Acknowledgements

The authors would like to show gratitude to CNPq for the financial aid given to this research.

6. References

[1] BARROS, J. A. O.; CRUZ, J. S.; ULRIX, E. "Avaliação da capacidade de absorção de energia de betões reforçados com fibras de aço". Journal of Experimental Mechanics of APAET, vol. 4, p. 1-11. Portugal, 1999.

[2] MAIDL, B. H. "Steel fiber reinforced concrete". 1st edition, Ernst & Sohn. Berlim, Alemanha, 1995.

[3] MARANGON, E. "Desenvolvimento e caracterização de concretos autoadensáveis reforçados com fibras de aço". Dissertação de Mestrado. COPPE, Universidade Federal do Rio de Janeiro. Rio de Janeiro, Brasil, 2006.

[4] LAPPA,E.S.; BRAAM , C.R.; WALRAVEN, J.C. "Bending Performance Of High Strength Steel Fibre Reinforced Concrete: Static and fatigue loading condition". Measuring, Monitoring and Modeling Concrete Properties, p. 133-138. Delft, Holanda, 2006.

[5] YAZICI, S.; INAN, G.; TABAK, V. "Effect of Aspect Ratio and Volume Fraction of Steel Fiber on the Mechanical Properties of SFRC". Construction and Building Materials, vol. 21, issue 6, p. 1250-1253. Izmir, Turquia, 2006.

[6] KARAHAN, O.; OZBAY, E.; ATIS, C.D; LACHEMI, M.; HOSSAIN, K.M.A. "Effects of Milled Cut Steel Fibers on the Properties of Concrete". KSCE Journal of Civil Engineering, vol. 20, issue 7, p. 2783-2789. Korea, 2016.

[7] WANG, Q.; LI, X.; ZhAO, G.; SHAO, P.; YAO, J. "Experiment on mechanical properties of steel fiber reinforced concrete and application in deep underground engineering". Journal of China University of Mining and Technology, vol. 18, issue 1, p. 64-66. China, 2008.

[8] TOLEDO FILHO, R. D.; MARANGON, E.; SILVA, F.A.; MOBASHER, B. "Effect of steel fibres on the tensile behaviour of self-consolidating reinforced concrete blocks". Fiber Reinforced Concrete: from Design to Structural Applications. American Concrete Institute Fib Workshop Proceedings, v. 79, p. 123-130. Montreal, Canadá, 2016.

[9] HERSCOVICI, H. L. "Estudo experimental de vigas curtas

de concreto com fibras de aço sujeitas à flexão". Dissertação de Mestrado. Pontifícia Universidade Católica do Rio de Janeiro, Rio de Janeiro, Brasil, 2016.

[10] ASSOCIAÇÃO BRASILEIRA DE NORMAS TÉCNICAS – NBR 7217: Agregados – Determinação da composição granulométrica. Rio de Janeiro, Brasil, 1987.

[11] ASSOCIAÇÃO BRASILEIRA DE NORMAS TÉCNICAS – NBR 9937: Agregados – Determinação da absorção e da massa específica de agregado graúdo. Rio de Janeiro, Brasil, 1987.

[12] AMERICAN SOCIETY FOR TESTING AND MATERIALS – ASTM C1018: Standard Test Method for Flexural Toughness and First-Crack Strength of Fiber-Reinforced Concrete (Using Beam with third-point loading). Estados Unidos, 1997.

[13] JAPAN SOCIETY OF CIVIL ENGINEERS – JSCE SF4: Steel Fiber 4 – Method of tests for flexural toughness of steel fiber reinforced concrete. Japão, 1984.

[14] CARPINTERI, A.; CHIAIA, B.; FERRO, G. "Size effects on nominal tensile of concrete structures: multifractality of material ligaments and dimensional transition form order to disorder". Materials and Structures, v. 28, p. 311-317. Torino, Itália, 1995.

[15] BARROS, J. A. O., "Comportamento do betão reforçado com fibras – análise experimental e simulação numérica". Tese de Doutorado. Faculdade de Engenharia da Universidade do Porto. Porto, Portugal, 1995.